© AUG 2026 | IRE Journals | Volume 10 Issue 2 | ISSN: 2456-8880
DOI: https://doi.org/10.64388/IREV10I2-1722449

Integrated Geophysical and Geochemical Characterization of Hydrocarbon Contamination at the Ajeokpori Artisanal Refinery Site, Ogale, Niger Delta, Nigeria

BRIGHT TAMUNOEMIGBAM OGOLO[1], TAMUNOENE KINGDOM SIMEON ABAM[2], PREYE K. NIMAME[3]
[1, 2, 3]Institute of Geosciences and Environmental Management, Rivers State University, Port-Harcourt, NIGERIA.

Abstract- Hydrocarbon contamination remains a major environmental and public health challenge in Ogoniland, Niger Delta, Nigeria, where legacy pollution and ongoing artisanal refining have complicated remediation planning. This study integrated geophysical, geochemical, and hydrogeological methods to delineate the extent of contamination at the Ajeokpori artisanal refinery site in Ogale, Eleme Local Government Area. Vertical Electrical Sounding using the Schlumberger array, 2D resistivity profiling using the Wenner array, 3D resistivity modeling, borehole logging, and laboratory analyses of soil and groundwater were combined to characterize subsurface conditions and contaminant migration. Eight VES points and fifteen boreholes were investigated, with a control site located 200 m upstream for comparison. Four geoelectric layers were identified to a maximum depth of 20.2 m, comprising silty sand topsoil, sandy silt, coarse sand, and medium sand. Contaminated-site resistivity ranged from 102 to 5860 Ω·m, while the control site ranged from 885 to 5100 Ω·m. Hydrocarbon-impacted zones were associated with low resistivity anomalies ≤700 Ω·m, which corresponded to elevated Total Petroleum Hydrocarbon concentrations ranging from 25 to 9,100 mg/kg. Groundwater TPH reached 8,050 µg/L, and plume migration followed southwestward groundwater flow in a high-permeability setting. A strong inverse relationship between soil resistivity and TPH concentration further supported the reliability of the integrated interpretation. The findings demonstrate that combined resistivity imaging and geochemical verification provide a robust basis for contamination delineation and remediation planning in hydrocarbon-impacted coastal plain aquifers.

Keywords: integrated, geophysical, geochemical, characterization, hydrocarbon contamination, niger delta

I. INTRODUCTION

Hydrocarbon pollution remains one of the most persistent environmental problems in the Niger Delta, where decades of petroleum exploitation, pipeline leakage, artisanal refining, and weak remediation have degraded soils and shallow aquifers. Ogoniland is among the most affected areas, and prior assessments have shown severe contamination of environmental media, including groundwater used for domestic purposes.

Recent site-characterization studies within the Niger Delta Coastal Plain Sands similarly show that crude-oil-impacted soils and shallow groundwater systems remain vulnerable where spills are not promptly remediated, as contaminants may infiltrate permeable sands and become concealed in the subsurface over time (Abam, Giadom, & Mogaba, 2025c; Abam, Giadom, & Mogaba, 2025d). This is particularly relevant in Ogoniland, where shallow unconfined aquifers, high permeability, and the historic pollution burden increase the need for reliable delineation before remedial action.

Ajeokpori in Ogale, Eleme Local Government Area, represents a particularly important case because the site combines legacy and active contamination pressures within a shallow, permeable coastal plain setting. In such environments, reliance on sparse soil sampling alone may underestimate the three-dimensional extent of contamination. An integrated approach that combines geophysical imaging with borehole and laboratory validation is therefore required to support reliable conceptual site modeling and remediation planning.

Hydrocarbon migration in such settings is controlled by surface topography, lithology, soil permeability, water-table variation, contaminant density, and seasonal recharge conditions. Light non-aqueous phase hydrocarbons generally spread laterally around the unsaturated-saturated interface or smear zone, while denser fractions may migrate vertically until constrained by less permeable horizons (Lesage & Jackson, 1992; United States Environmental Protection Agency [US EPA], 2010; Abam, Giadom, & Mogaba, 2025d).

Electrical resistivity methods have become valuable tools in environmental site characterization because they permit non-intrusive delineation of subsurface heterogeneity and contaminant distribution. However, their interpretation is strongest when calibrated against direct geochemical evidence. This study therefore aimed to integrate vertical electrical sounding, resistivity profiling, 3D modeling, borehole logging, and geochemical analysis to delineate hydrocarbon contamination at the Ajeokpori artisanal refinery site and to provide data relevant to remediation planning.

In aged hydrocarbon-impacted sands, biodegradation, organic-acid generation, and increased dissolved solids may transform the geoelectrical response from a high-resistivity signature typical of fresh product to low-resistivity anomalies in mature spills (Sauck, 1998, 2000; Atekwana, Sauck, & Werkema, 2000). For this reason, resistivity thresholds are best treated as site-specific and constrained by borehole and geochemical evidence rather than applied as universal limits.

II. MATERIALS AND METHODS

The study was conducted at the Ajeokpori artisanal refinery site in Ogale, Eleme LGA, Rivers State, Nigeria, within the Benin Formation of the Niger Delta Basin.

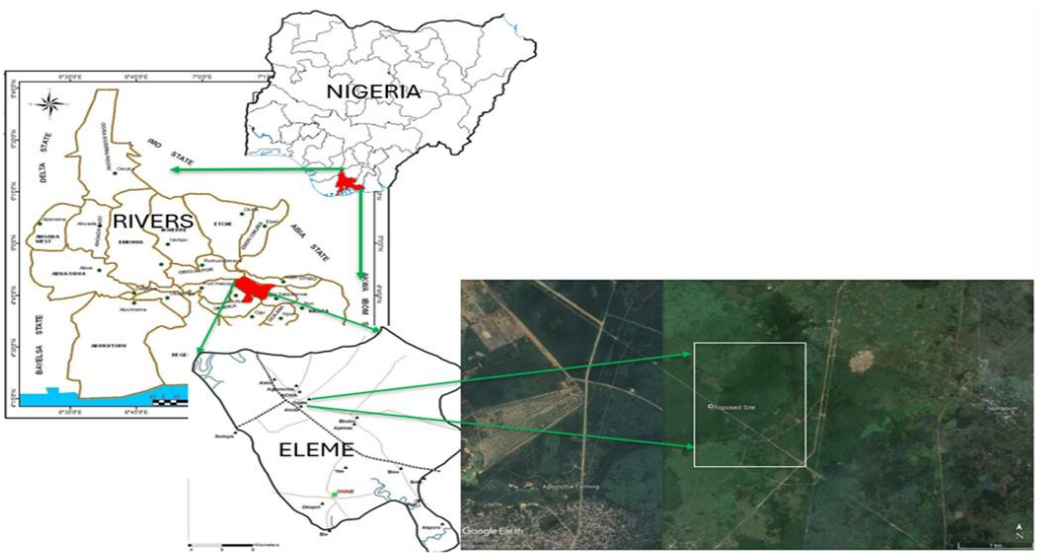

Fig.1 The study area lies in Ajeokpori, Ogale community, Eleme L.G.A, Rivers State and is bounded by 4°49’2.00"N and 4°49'34.00"Nand longitudes 7° 8’5.00"E and 7° 8’57.00"E. This area was identified in the UNEP report as severely contaminated.

The subsurface is dominated by sandy and silty materials that function as an unconfined aquifer system and are highly vulnerable to hydrocarbon infiltration. A control site located 200 m upstream was investigated to provide baseline conditions.

The site conceptual model followed the environmental logic applied in recent Ogoni ERI/ERT investigations: surface relief and suspected source locations guided the expected plume trajectory, while direct borehole evidence was used to confirm whether low-resistivity zones reflected hydrocarbon impact rather than lithological effects such as clay-rich horizons (Abam, Giadom, Mogaba, & Nwankwo, 2025b; Abam, Giadom, & Mogaba, 2025c).

The investigation integrated geophysical, borehole, geochemical, and hydrogeological datasets. Vertical Electrical Sounding was conducted using the Schlumberger array to evaluate vertical resistivity variation and contamination depth. Horizontal resistivity profiling was carried out using the Wenner array to image lateral plume extent, and the 2D outputs were subsequently modeled in three dimensions. A total of eight VES points and fifteen boreholes were analyzed within the contaminated area, with corresponding control-site observations used for comparison.

Borehole data were used to validate geophysical interpretation and characterize lithologic units. Soil and groundwater samples were analyzed for Total Petroleum Hydrocarbon, while selected analyses also covered Polycyclic Aromatic Hydrocarbons and BTEX compounds. Hydrogeological assessment included groundwater level evaluation, groundwater flow interpretation, and hydraulic conductivity estimation. The combined data were interpreted to delineate contamination extent, identify plume migration trends, and support remediation planning. Human health risk was assessed separately using established exposure models, but that analysis is outside the main focus of this paper.

Accordingly, resistivity sections were interpreted together with borehole observations, laboratory TPH, PAH and BTEX results, and groundwater-level data. This integrated approach reduces the uncertainty associated with intrusive sampling alone and improves the reliability of contaminant boundary mapping, remediation-area estimation, and monitoring-well placement.

III. RESULTS

The geophysical investigation identified four geoelectric layers to a maximum depth of 20.2 m.

Table 1: Summary of VES model, showing resistivity values, depth, thickness, and oil-contaminated geo-electric layers for study area.

Line No	No of Layer(s)	Resistivity (Ohm.m)	Depth (m)	Thickness (m)	Lithology
VES_1	1	2010	0.51	0.51	Silty Sand Topsoil
	2	433	3.55	3.04	Oil Contaminated Layer
	3	332	7.51	3.96	Oil Contaminated Layer
	4	1230	20.2	12.7	Medium Sand
VES_2	1	1560	0.45	0.45	Silty Sand Topsoil
	2	300	3.55	3.1	Oil Contaminated Layer
	3	210	7.45	3.9	Oil Contaminated Layer
	4	1100	20.1	12.7	Medium Sand
VES_3	1	3211	0.45	0.45	Silty Sand Topsoil
	2	1108	3.4	2.95	Sandy Silt
	3	5860	7.2	3.8	Coarse Sand
	4	1001	20.1	12.9	Medium Sand
VES_4	1	179	0.55	0.55	Oil Contaminated Layer
	2	230	3.58	3.03	Oil Contaminated Layer
	3	550	7	3.42	Oil Contaminated Layer
	4	350	20	13	Oil Contaminated Layer
VES_5	1	3800	0.58	0.58	Silty Sand Topsoil
	2	1670	3.45	2.87	Sandy Silt
	3	5100	7.5	4.05	Coarse Sand
	4	1200	20.2	12.7	Silty Sand
VES_6	1	321	0.48	0.48	Oil Contaminated Layer

	2	223	3.33	2.85	Oil Contaminated Layer
	3	102	7.5	4.17	Oil Contaminated Layer
	4	311	19.9	12.4	Oil Contaminated Layer
VES_7	1	4001	0.52	0.52	Silty Sand Topsoil
	2	1800	3.65	3.13	Sandy Silt
	3	5101	7.6	3.95	Medium Sand
	4	1460	20.1	12.5	Coarse Sand
VES_8	1	218	0.5	0.5	Oil Contaminated Layer
	2	202	3.5	3	Oil Contaminated Layer
	3	5005	7.5	4	Medium Sand
	4	1332	20	12.5	Coarse Sand
VES_9	1	3210	0.54	0.54	Silty Sand Topsoil
	2	2300	3.56	3.02	Sandy Silt
	3	5100	7.56	4	Coarse Sand
	4	885	20.2	12.6	Medium Sand (Aquifer)

Lithologies encountered included silty sand topsoil, sandy silt, coarse sand, and medium sand. Resistivity values in the contaminated area ranged from 102 to 5860 Ω·m, compared with 885 to 5100 Ω·m at the control site. Interpreted geoelectric sections were consistent with borehole lithologic logs.

Hydrocarbon contamination was associated with low resistivity anomalies of ≤700 Ω·m.
The adopted ≤700 Ω·m operational cutoff agrees with the range of locally calibrated thresholds reported for hydrocarbon-impacted Coastal Plain Sands, including values of ≤550 to ≤700 Ω·m in recent Ogoni investigations. Its use at Ajeokpori is therefore supported by local geophysical precedent, but more importantly by the independent borehole evidence and elevated TPH concentrations obtained in this study (Abam, Giadom, Mogaba, & Nwankwo, 2025b; Abam, Giadom, & Mogaba, 2025c; Abam, Giadom, & Mogaba, 2025d).

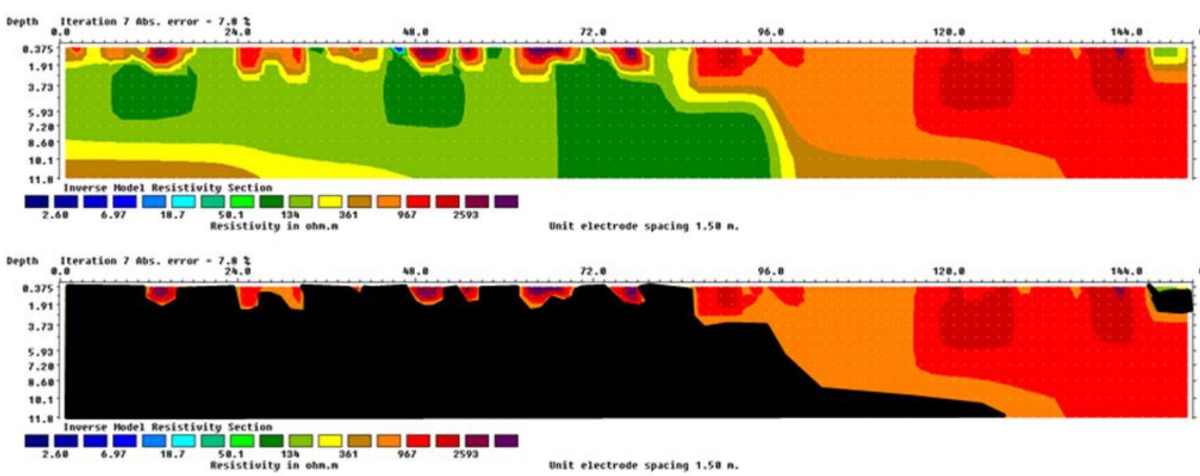

Fig 2. Representative 2D resistivity tomogram: Processed electrical resistivity tomogram for Line 1 using RES2DINV software (dark area highlighted on second tomogram shows oil contaminated zones with resistivity values ≤700 Ωm)

DOI: https://doi.org/10.64388/IREV10I2-1722449

Soil geochemistry confirmed extensive contamination, with TPH concentrations ranging from 25 to 9,100 mg/kg and several samples exceeding the DPR intervention limit of 5,000 mg/kg.

Table 2: Summary of key geochemical indicators in soil and groundwater across the study area with DPR regulatory benchmarks

Parameter	Medium	Range	Mean	No. exceeding DPR target	No. exceeding DPR intervention	Key maximum value(s) / hotspot(s)	DPR target	DPR intervention
Total Petroleum Hydrocarbon (TPH)	Soil (mg/kg)	1.1-9100	1594.02	38/80	5/80	9100 mg/kg at BH4 (5 m); 8900 mg/kg at BH4 (2 m); 8500 mg/kg at BH7 (3 m); 8100 mg/kg at BH7 (5 m)	50	5000
Polycyclic Aromatic Hydrocarbon (PAH)	Soil (mg/kg)	0.8-7.53	2.74	12/80	0/80	7.53 mg/kg at BH4 (2 m); 5.85 mg/kg at BH4 (5 m); 3.80 mg/kg at BH1 (2 m)	1	40
Total Petroleum Hydrocarbon (TPH)	Groundwater (ug/L)	<10-8050	1971.54	12/15	8/15	8050 ug/L at BH4; 5550 ug/L at BH7; 4500 ug/L at BH15	50	600

1. Soil TPH and PAH values were summarized from the borehole datasets at depths of 0.5, 2, 3, 5, 7, and 10 m across the study area. Groundwater TPH values were summarized from boreholes BH1 to BH15.
2. DPR = Department of Petroleum Resources (2002) regulatory guideline values for contaminated soil and groundwater in Nigeria.
3. Reported ranges and means were derived from the detected numerical values presented in the dataset. Entries reported as below detection limit, such as <10, <0.8, and <0.5, were retained as non-detect observations in interpretation.
4. 'No. exceeding target/intervention limit' refers to the number of reported observations above the corresponding DPR threshold.
5. The highest soil TPH and PAH values were recorded around BH4 and BH7, while the highest groundwater TPH concentrations occurred at BH4, BH7, and BH15, indicating these as major contamination hotspots within the study area.

© AUG 2026 | IRE Journals | Volume 10 Issue 2 | ISSN: 2456-8880
DOI: https://doi.org/10.64388/IREV10I2-1722449

PAHs were detected at concentrations up to 7.53 mg/kg, while BTEX occurrence indicated the persistence of residual free-phase hydrocarbons. Groundwater analysis indicated TPH concentrations as high as 8,050 µg/L, suggesting that subsurface pollution had migrated into the shallow aquifer.

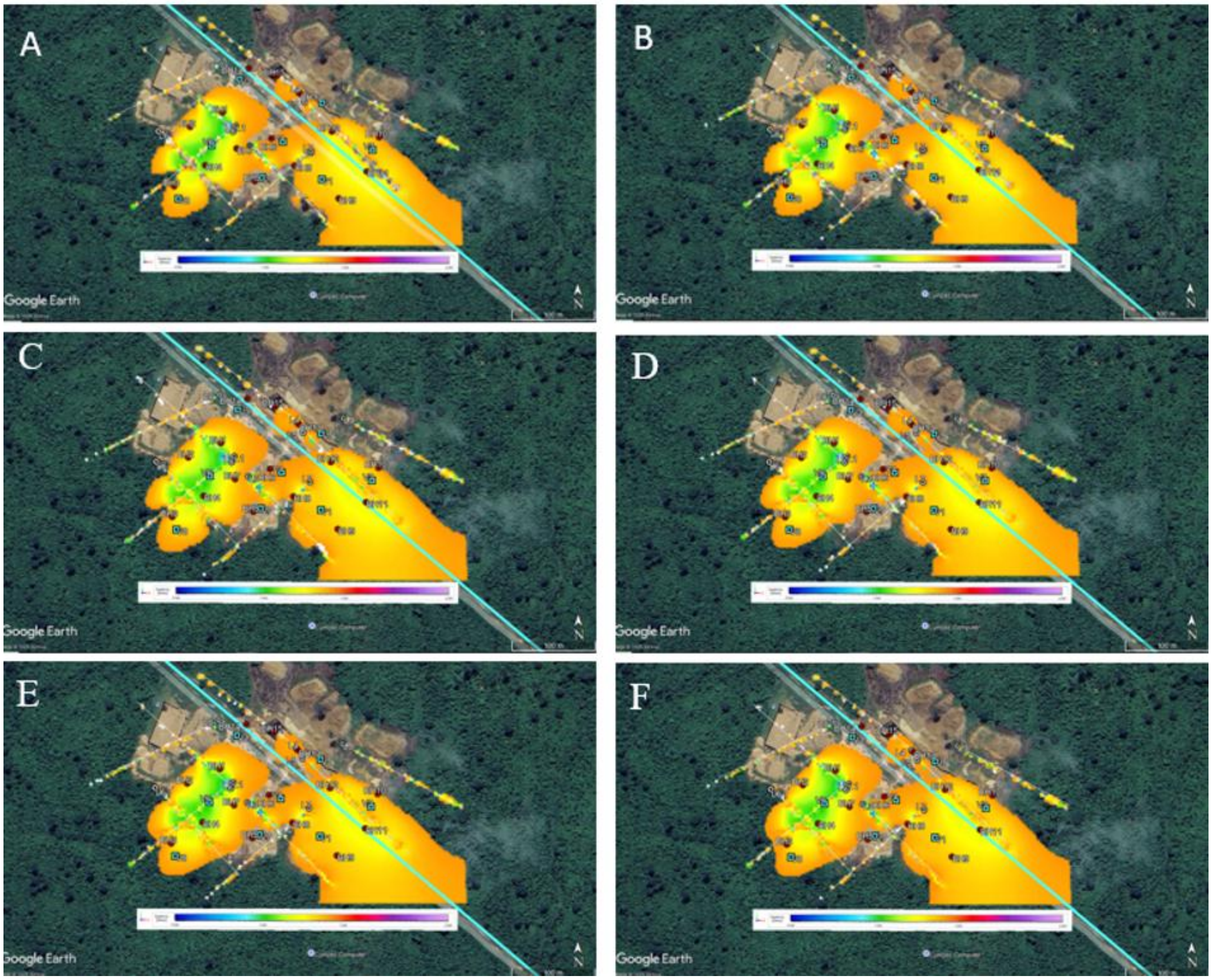

Fig 3. 3D contamination/plume map: Resistivity models overlaid on google map after applying a resistivity cut-off for oil contamination at ≤700 Ohm.m. (a) 1.0m (b) 3.0m (c) 5.0m (d) 7.0m (e) 10.0m (f) 13.0m

Groundwater flow was directed toward the southwest, and plume geometry derived from geophysical mapping was consistent with geochemical patterns observed in the borehole TPH data.

© AUG 2026 | IRE Journals | Volume 10 Issue 2 | ISSN: 2456-8880
DOI: https://doi.org/10.64388/IREV10I2-1722449

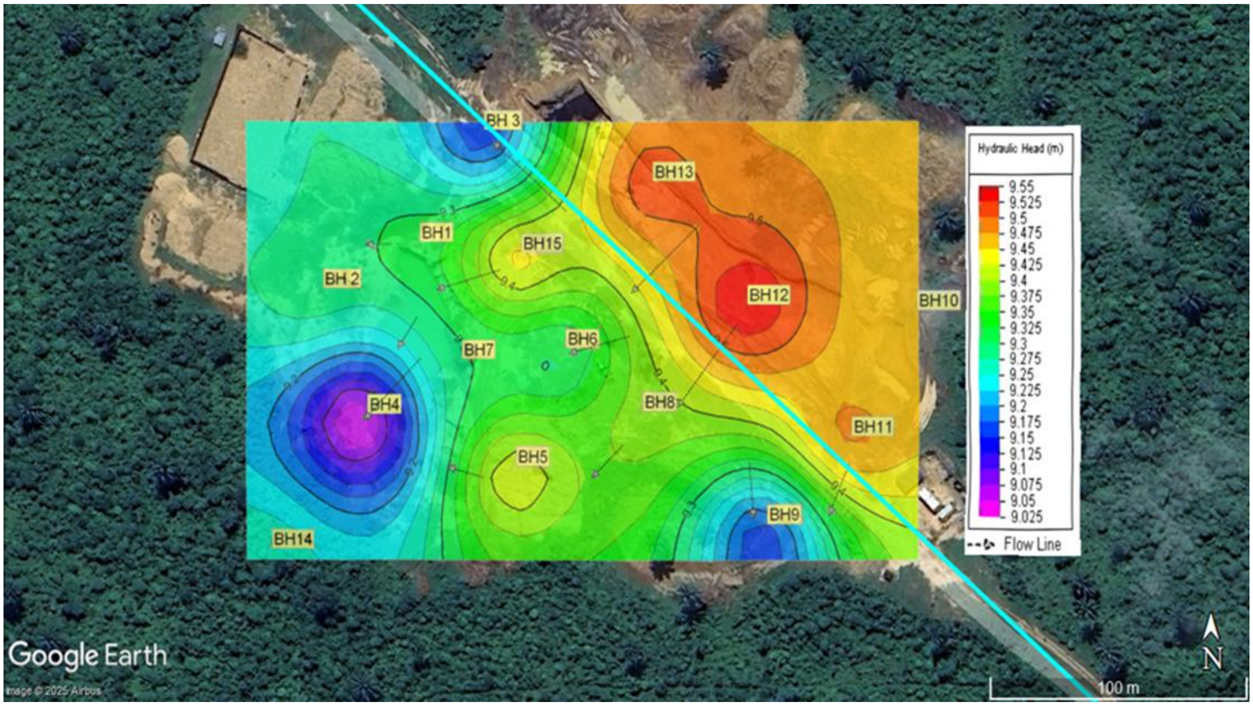

Fig.5. Map showing groundwater flow direction

Average hydraulic conductivity of 1.28 m/day suggested favorable conditions for contaminant migration along flow paths.

Table 3. Compact summary of groundwater level conditions and hydraulic conductivity across the study area

Parameter	Range	Mean	Key extrema / compact interpretation
Surface elevation (masl)	11.59-13.41	12.18	Highest at BH9 (13.41 masl); lowest at BH7 (11.59 masl).
Static water level, SWL (mbgl)	2.19-4.29	2.84	Deepest water table at BH9 (4.29 mbgl); shallowest at BH15 (2.19 mbgl).
Hydraulic head (masl)	8.98-9.57	9.34	Highest head at BH12 (9.57 masl) and lowest at BH4 (8.98 masl), indicating a subdued hydraulic gradient across the site.
Hydraulic conductivity, Cooper et al. (1967) (m/day)	0.398-1.62	1.13	Lowest at BH8 (0.398 m/day); highest at BH14 (1.62 m/day).

© AUG 2026 | IRE Journals | Volume 10 Issue 2 | ISSN: 2456-8880
DOI: https://doi.org/10.64388/IREV10I2-1722449

Hydraulic conductivity, Hvorslev (1951) (m/day)	0.432-1.97	1.19	Lowest at BH8 (0.432 m/day); highest at BH10 (1.97 m/day).
Average hydraulic conductivity (m/day)	0.415-1.73	1.16	Overall average is 1.16 m/day. Highest average K occurs at BH10 (1.73 m/day) and lowest at BH8 (0.415 m/day), suggesting generally moderate to relatively high permeability with local variability.

Notes: masl = metres above sea level; mbgl = metres below ground level. Hydraulic head was computed as elevation minus static water level. Hydraulic conductivity values were summarized from slug-test results using the Cooper et al. (1967) and Hvorslev (1951) methods.

Overall, the hydraulic head distribution and the moderate-to-high hydraulic conductivity values suggest that the shallow subsurface permits lateral migration of petroleum contaminants. This interpretation is in agreement with the spatial distribution of elevated TPH concentrations in soil and groundwater, from which the maximum contaminated area requiring remediation was delineated as 6566.23 m².

Cross-plot analysis demonstrated a strong inverse relationship between soil TPH concentration and soil resistivity, with the fitted trend indicating a strong relationship ($R^2 \approx 0.8112$).

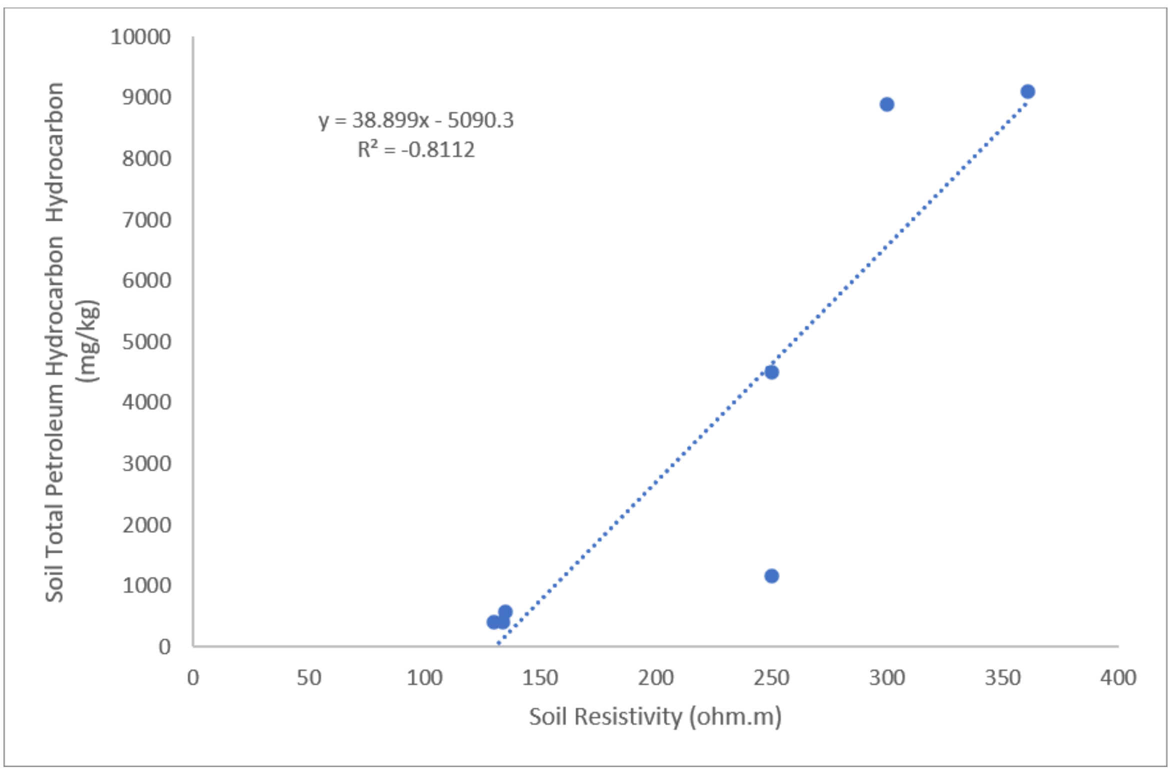

Figure 4: Cross-plot of soil TPH versus soil resistivity.

This indicates that higher hydrocarbon loading corresponded to lower resistivity signatures in the contaminated zone.

IV. DISCUSSION

The results show that integrated resistivity imaging and geochemical verification provide a robust framework for characterizing hydrocarbon-impacted sites in sandy coastal plain environments. The low-resistivity threshold identified in this study is particularly important because it offers an operational basis for mapping contaminated zones where field access is limited and borehole spacing alone would not provide sufficient spatial resolution.

This interpretation is consistent with earlier Niger Delta and international hydrogeophysical studies which show that mature hydrocarbon plumes in sandy aquifers commonly develop conductive anomalies as microbial degradation produces leachates and increases total dissolved solids around impacted zones. Consequently, the low-resistivity signature at Ajeokpori is best interpreted as a mature contamination response where it coincides with hydrocarbon odour, borehole evidence, and elevated TPH concentrations, rather than as a stand-alone lithological indicator.

The agreement between resistivity anomalies, borehole logs, and TPH concentrations strengthens confidence in the site interpretation. In practical terms, this means that geophysical methods can substantially improve contamination delineation when used alongside direct soil and groundwater analyses rather than as stand-alone tools. This is especially relevant in Ogoniland, where remediation planning requires site-specific plume geometry rather than broad regional assumptions.

The hydrogeological setting further explains the seriousness of the site condition. The shallow, permeable aquifer and southwestward groundwater flow indicate an active pathway for contaminant migration, increasing the risk of continued groundwater deterioration if remediation is delayed. The measured hydraulic conductivity supports this interpretation and suggests that plume movement is not static.

The role of groundwater-level fluctuation is also important. Buoyant petroleum fractions may persist around the smear zone during seasonal rise and fall of the water table, while groundwater flow controls the direction of dissolved-phase transport. This supports continued downgradient groundwater monitoring and makes delayed remediation environmentally risky.

From a remediation standpoint, the study provides decision-support information that is more actionable than contamination confirmation alone. The delineated impacted area, validated plume direction, and correlation between resistivity and hydrocarbon concentrations can all inform the targeting of remedial intervention, monitoring locations, and verification programs.

Consequently, remediation at Ajeokpori should be designed around confirmed hotspots and plume geometry rather than broad excavation assumptions. Priority should be given to the BH4, BH7, and BH15 hotspot areas, downgradient monitoring, and post-remediation verification using repeat resistivity imaging supported by confirmatory soil and groundwater analyses.

V. CONCLUSION

The Ajeokpori artisanal refinery site is significantly impacted by hydrocarbon contamination in both soil and groundwater. Integrated geophysical and geochemical analysis successfully delineated the vertical and lateral extent of contamination and demonstrated that low resistivity anomalies correspond to elevated hydrocarbon concentrations. The shallow aquifer setting, southwestward groundwater flow, and measured contaminant levels indicate a site requiring urgent remediation and continued monitoring. This integrated framework is suitable for supporting risk-based remediation planning in Ogoniland and similar hydrocarbon-impacted environments.

The reviewed literature further supports the position that ERT/ERI is most reliable when used within an integrated framework, with site-specific resistivity thresholds calibrated by borehole, geochemical, and hydrogeological evidence. For remediation planning, this study recommends targeted intervention around confirmed hotspots, continued monitoring along southwestward flow paths, and repeat geophysical-geochemical verification to track remedial effectiveness.

REFERENCES

[1] Abam, T. K. S., Giadom, F. D., Mogaba, P. M., & Nwankwo, I. L. (2025a). Comparison of RES2DINV and Earth Imager tomography with litho-ground models of hydrocarbon contaminated site in the Coastal Plain Sand of Niger Delta. Journal of Mining and Geology, 60(2).

[2] Abam, T. K. S., Giadom, F. D., Mogaba, P. M., & Nwankwo, I. L. (2025b). Electrical resistivity imaging and lithological modelling of hydrocarbon contaminated soil in Ogoni, Rivers State, Nigeria. International Journal of Research and Innovation in Applied Science, 10(6), 58-68. https://doi.org/10.51584/IJRIAS.2025.10060005

[3] Abam, T. K. S., Giadom, F. D., & Mogaba, P. M. (2025c). Site characterization and delineation of hydrocarbon-contaminated area within the Coastal Plain sand using the qualitative and non-intrusive ERT method, Rivers State, Nigeria. Global Scientific Journal, 13(8), 1468-1482.

[4] Abam, T. K. S., Giadom, F. D., & Mogaba, P. M. (2025d). Spatial and vertical distribution of hydrocarbon contamination in Coastal Plain Sands of the Niger Delta, Nigeria. International Journal of Latest Technology in Engineering, Management & Applied Science, 14(8), 1277-1283. https://doi.org/10.51583/IJLTEMAS.2025.1408000164

[5] Ahmed, N. O., Nik Daud, N. N., & Okunlola, I. A. (2024). Geoelectrical soil mapping for subsurface hydrocarbon contaminant characterization and remediation site zoning at Alode, Central Niger Delta, Nigeria. Environmental Technology & Innovation. https://doi.org/10.1016/j.eti.2024.103935

[6] Aizebeokhai, A. P. (2010). 2D and 3D geoelectrical resistivity imaging: Theory and field design. Scientific Research and Essays, 5(23), 3592-3605.

[7] Atekwana, E. A., Sauck, W. A., & Werkema, D. D. (2000). Investigations of geoelectrical signatures at a hydrocarbon contaminated site. Journal of Applied Geophysics, 44(2-3), 167-180. https://doi.org/10.1016/S0926-9851(98)00033-0

[8] Ayolabi, E. A., Folorunso, A. F., & Idem, S. S. (2013). Application of electrical resistivity tomography in mapping subsurface hydrocarbon contamination. Earth Science Research, 2(1), 93-104. https://doi.org/10.5539/esr.v2n1p93

[9] Binley, A., & Kemna, A. (2005). DC resistivity and induced polarization methods. In Y. Rubin & S. S. Hubbard (Eds.), Hydrogeophysics (pp. 129-156). Springer. https://doi.org/10.1007/1-4020-3102-5_5

[10] Department of Petroleum Resources. (2002). Environmental guidelines and standards for the petroleum industry in Nigeria (EGASPIN). Department of Petroleum Resources.

[11] Ehirim, C. N., Adizua, O. F., & Okorie, I. P. C. (2016). Geoelectrical characterization of matured petroleum hydrocarbon impacted soil in Port Harcourt, Nigeria. Asian Journal of Earth Sciences, 9, 9-15. https://doi.org/10.3923/ajes.2016.9.15

[12] Eze, S. U., Ogagarue, D. O., Nnorom, S. L., et al. (2021). Integrated geophysical and geochemical methods for environmental assessment of subsurface hydrocarbon contamination. Environmental Monitoring and Assessment, 193, Article 451. https://doi.org/10.1007/s10661-021-09219-3

[13] Lesage, S., & Jackson, R. E. (1992). Groundwater contamination and analysis at hazardous waste sites. Marcel Dekker.

[14] Loke, M. H., & Barker, R. D. (1996). Rapid least-squares inversion of apparent resistivity pseudosections by a quasi-Newton method. Geophysical Prospecting, 44(1), 131-152. https://doi.org/10.1111/j.1365-2478.1996.tb00142.x

[15] Reynolds, J. M. (2011). An introduction to applied and environmental geophysics (2nd ed.). Wiley-Blackwell.

[16] Sauck, W. A. (1998). A conceptual model for the geoelectrical response of LNAPL plumes in

granular sediments. In Proceedings of the Symposium on the Application of Geophysics to Engineering and Environmental Problems (SAGEEP) (pp. 805-817). Environmental and Engineering Geophysical Society.

[17] Sauck, W. A. (2000). A model for the resistivity structure of LNAPL plumes and their environs in sandy sediments. Journal of Applied Geophysics, 44(2-3), 151-165.

[18] Shevnin, V., Delgado-Rodríguez, O., Mousatov, A., Nakamura-Labastida, E., & Mejía-Aguilar, A. (2003). Oil pollution detection using resistivity sounding. Geofísica Internacional, 42(4), 613-622.

[19] Tse, A. C., & Nwankwo, A. C. (2013). An integrated geochemical and geoelectrical investigation of an ancient crude oil spill site in south east Port Harcourt, Southern Nigeria. Ife Journal of Science, 15(1), 127-140.

[20] United Nations Environment Programme. (2011). Environmental assessment of Ogoniland. UNEP.

[21] United States Environmental Protection Agency. (2010). Waste and cleanup risk assessment glossary. US EPA.